

Two Lectures on DMRG in Quantum Chemistry

Markus Reiher

Laboratorium für Physikalische Chemie, ETH Zürich, Switzerland

<http://www.reiher.ethz.ch>

June 2015

Two Lectures on DMRG in Quantum Chemistry

- 1 First-Generation Density Matrix Renormalization Group (DMRG) in Quantum Chemistry
- 2 Second-Generation DMRG:
Matrix Product and Tensor Network States
Matrix Product Operators
- 3 Some Results of Actual Quantum-Chemical Calculations

Very useful introductory reference:

U. Schollwöck, *The density-matrix renormalization group in the age of matrix product states*, arXiv: 1008.3477v2

Reviews on DMRG in Quantum Chemistry

- 1 Ö Legeza, R. M. Noack, J. Sólyom and L. Tincani, Applications of Quantum Information in the Density-Matrix Renormalization Group, Lect. Notes Phys., 739,653-664 (2008)
- 2 G. K.-L. Chan, J. J. Dorando, D. Ghosh, J. Hachmann, E. Neuscamman, H. Wang, T. Yanai, An Introduction to the Density Matrix Renormalization Group Ansatz in Quantum Chemistry, Prog. Theor. Chem. and Phys., 18, 49 (2008)
- 3 D. Zgid and G. K.-L. Chan, The Density Matrix Renormalisation Group in Quantum Chemistry, Ann. Rep. Comp. Chem., 5, 149, (2009)
- 4 K. H. Marti, M. Reiher, The Density Matrix Renormalization Group Algorithm in Quantum Chemistry, Z. Phys. Chem., 224, 583-599 (2010)
- 5 G. K.-L. Chan and S. Sharma, The density matrix renormalization group in quantum chemistry, Ann. Rev. Phys. Chem., 62, 465 (2011)
- 6 K. H. Marti, M. Reiher, New Electron Correlation Theories for Transition Metal Chemistry, Phys. Chem. Chem. Phys., 13, 6750-6759 (2011)
- 7 Y. Kurashige, Multireference electron correlation methods with density matrix renormalisation group reference functions, Mol. Phys. 112, 1485-1494 (2014)
- 8 S. Wouters and D. Van Neck, The density matrix renormalization group for ab initio quantum chemistry, Eur. Phys. J. D 68, 272 (2014)
- 9 T. Yanai, Y. Kurashige, W. Mizukami, J. Chalupský, T. N. Lan, M. Saitow, Density matrix renormalization group for ab initio Calculations and associated dynamic correlation methods, Int. J. Quantum Chem. 115, 283-299 (2015)
- 10 S. Szalay, M. Pfeffer, V. Murg, G. Barcza, F. Verstraete, R. Schneider, Ö. Legeza, Tensor product methods and entanglement optimization for ab initio quantum chemistry, arXiv:1412.5829 (2015)

Lecture 1

First-Generation DMRG in Quantum Chemistry

- 1 Standard Configuration Interaction in Explicit Second Quantization
- 2 Dimension Reduction by Decimation
- 3 Elements of the DMRG Algorithm

Non-Relativistic Many-Electron Hamiltonian

- many-electron **Hamiltonian** in position space (Hartree atomic units)

$$H_{el} = \sum_i^N \left(-\frac{1}{2} \nabla_i^2 - \sum_I \frac{Z_I}{r_{iI}} \right) + \sum_{i < j}^N \frac{1}{r_{ij}} \quad (1)$$

with $r_{ij} = |\mathbf{r}_i - \mathbf{r}_j|$ and N being the number of electrons.

- eigenvalue equation: electronic Schrödinger equation

$$H_{el} \Psi_{el}^{\{\mathbf{R}_I\}}(\{\mathbf{r}_i\}) = E_{el}(\{\mathbf{R}_I\}) \Psi_{el}^{\{\mathbf{R}_I\}}(\{\mathbf{r}_i\}) \quad (2)$$

- central in electronic structure theory: how to approximate Ψ_{el} ?

Standard Procedure: Construction of Many-Electron Basis

- Construct many-electron (determinantal) basis set $\{\Phi_I\}$ from a given (finite) one-electron (orbital) basis set ϕ_i
- From the solution of the Roothaan–Hall equations, one obtains n orbitals from n one-electron basis functions.
- From the N orbitals with the lowest energy, the Hartree–Fock (HF) Slater determinant is constructed.
- The other determinants (configurations) are obtained by subsequent substitution of orbitals in the HF Slater determinant Φ_0 :

$$\{\Phi_I\} \rightarrow \Phi_i^a, \Phi_j^b, \dots \rightarrow \Phi_{ij}^{ab}, \Phi_{ik}^{ac}, \dots \rightarrow \Phi_{ijk}^{abc}, \Phi_{ijl}^{abd}, \dots \quad (3)$$

- Determinants are classified by number of 'excitations' (= substitutions in HF reference determinant).

Standard Full Configuration Interaction (FCI)

- The number of possible determinants is determined by the number of virtual orbitals $n - N$.
- Including all possible excited Slater determinants for a finite or infinite one-electron basis set leads to the so-called **full CI** approach.
- Number of Slater determinants n_{SD} for N spin orbitals chosen from a set of n spin orbitals (slang: N electrons in n spin orbitals):

$$n_{\text{SD}} = \binom{n}{N} = \frac{n!}{N!(n - N)!} \quad (4)$$

Example: There are $\approx 10^{12}$ different possibilities to distribute 21 electrons in 43 spin orbitals.

- *In physics FCI is called exact diagonalization.*

Truncated CI Wave Functions

Standard recipe to avoid the factorial scaling of the many-electron basis-set size: **truncate basis!** *Note: basis is pre-defined!*

Assumption: Substitution hierarchy is a useful measure to generate a systematically improvable basis set.

CIS: all singly-(S)-excited determinants are included:

$$\Psi_{el}^{CIS} = C_0 \Phi_0 + \sum_{(ai)} C_{(ai)} \Phi_i^a \quad (5)$$

CISD: all singly- and doubly-(D)-excited determinants are included:

$$\Psi_{el}^{CISD} = C_0 \Phi_0 + \sum_{(ai)} C_{(ai)} \Phi_i^a + \sum_{(ai)(bj)} C_{(ai,bj)} \Phi_{ij}^{ab} \quad (6)$$

$$C_0, C_{(ai)}, C_{(ai,bj)} \in \{C_I\} \quad (7)$$

Determination of the CI Expansion Coefficients C_I

The CI expansion coefficients C_I determined by variational principle:

- write down the expectation value for the energy
- introduce the determinantal basis set
- vary the energy in order to minimize it

Expectation value for the CI electronic energy:

$$E_{el}^{CI} = \frac{\langle \Psi_{el}^{CI} | H_{el} | \Psi_{el}^{CI} \rangle}{\langle \Psi_{el}^{CI} | \Psi_{el}^{CI} \rangle} \quad (8)$$

Insert expansion of Slater determinants:

$$E_{el}^{CI} = \frac{\sum_{K,L} C_K^* C_L \langle \Phi_K | H_{el} | \Phi_L \rangle}{\sum_{K,L} C_K^* C_L \langle \Phi_K | \Phi_L \rangle} \quad (9)$$

The CI Eigenvalue Problem

Calculate all derivatives $\partial E_{el}^{CI} / \partial C_K^*$ and set them equal to zero, which yields the **CI eigenvalue problem**:

$$H \cdot C = E_{el} \cdot C \quad (10)$$

Essential: H is constructed from matrix elements $\langle \Phi_K | H_{el} | \Phi_L \rangle$ in the pre-defined determinantal basis $\{\Phi_K\}$

By solving the CI eigenvalue problem, ground and excited electronic states of the system are obtained.

E_{el} is diagonal matrix with total energies of all electronic states that can be expressed in basis given (M determinants yield M electronic states).

Standard 'Technical' Trick: Second Quantization

Operators and wave functions are expressed in terms of creation and annihilation operators to implement the Slater–Condon rules for the evaluation of matrix elements $\langle \Phi_K | H_{el} | \Phi_L \rangle$ directly into the formalism.

H_{el} in second quantization (i, j, k, l are spin orbital indices):

$$\Rightarrow H_{el} = \sum_{ij} \langle \phi_i | h(i) | \phi_j \rangle a_i^\dagger a_j + \frac{1}{2} \sum_{ijkl} \langle \phi_i(1) \phi_k(2) | g(1,2) | \phi_l(2) \phi_j(1) \rangle a_i^\dagger a_j^\dagger a_k a_l \quad (11)$$

CI wave function in second quantization:

$$\Psi_{el}^{\text{FCI}} = C_0 \Phi_0 + \sum_{(ai)} C_{(ai)} a_a^\dagger a_i \Phi_0 + \sum_{(ai)(bj)} C_{(ai,bj)} a_b^\dagger a_j a_a^\dagger a_i \Phi_0 \cdots \quad (12)$$

CI Energy in Second Quantization

$$E_{el}^{CI} = \left\langle \Psi_{el}^{CI} \left| H_{el} \right| \Psi_{el}^{CI} \right\rangle \quad (13)$$

$$= \sum_{ij}^N \underbrace{\sum_{KL}^N C_K^* C_L t_{ij}^{KL}}_{\gamma_{ij}} \underbrace{\langle \phi_i(1) | h(1) | \phi_j(1) \rangle}_{\equiv h_{ij}} \\ + \sum_{ijkl}^N \underbrace{\sum_{KL}^N C_K^* C_L T_{ijkl}^{KL}}_{\Gamma_{ijkl}} \underbrace{\langle \phi_i(1) \langle \phi_k(2) | g(1,2) | \phi_l(2) \rangle \phi_j(1) \rangle}_{g_{ijkl}} \quad (14)$$

$$= \sum_{ij}^N \gamma_{ij} h_{ij} + \sum_{ijkl}^N \Gamma_{ijkl} g_{ijkl} \quad (15)$$

t_{ij}^{KL} or T_{ijkl}^{KL} are matrix elements of determinantal basis functions over pairs or quadruples of elementary operators a^\dagger and a .

γ_{ij} are Γ_{ijkl} are density matrix elements.

Is there a better way to construct the finite-dimensional determinantal basis set in order to avoid the factorial scaling?

Coupled-Cluster — An Advanced CI-type Wave Function

Ansatz:

$$\Psi_{\text{el}}^{\text{CC}} = \exp(T) \Phi_{\text{el}}^{\text{HF}} \quad (16)$$

Excitation operator:

$$T = T_1 + T_2 + T_3 + \dots \quad (17)$$

where

$$T_\alpha = \sum_{\underbrace{ab \dots}_{\alpha \text{ times}} \underbrace{ij \dots}_{\alpha \text{ times}}} \overbrace{t_{ij\dots}^{ab\dots}}^{\text{cluster-amplitudes}} \underbrace{\dots a_b^\dagger a_j a_a^\dagger a_i}_{\substack{\alpha \text{ pairs} \quad a^\dagger a}} \Rightarrow T_1 = \sum_{ai} t_i^a a_a^\dagger a_i \quad (18)$$

Notation:

CCS ($T = T_1$), CCSD ($T = T_1 + T_2$), CCSDT ($T = T_1 + T_2 + T_3$), \dots

Coupled-cluster improves on truncated CI, because certain (disconnected) higher excited configurations (e.g., $t_i^a a_a^\dagger a_i t_{jk}^{bc} a_c^\dagger a_k a_b^\dagger a_j$) are included.

Is there a better way to construct the finite-dimensional determinantal basis set in order to avoid the factorial scaling?

Let's investigate FCI from a different perspective:

Many-Electron Hamiltonian in Second Quantization

- many-electron **Hamiltonian** in second quantization

$$H_{el} = \sum_{\substack{i,j \\ \sigma}} h_{ij} a_{i\sigma}^\dagger a_{j\sigma} + \frac{1}{2} \sum_{\substack{i,j,k,l \\ \sigma,\sigma'}} V_{ijkl} a_{i\sigma}^\dagger a_{j\sigma'}^\dagger a_{k\sigma'} a_{l\sigma} \quad (19)$$

with $\sigma \in \{\alpha, \beta\}$ and the creators and annihilators $a_{i\sigma}$ and $a_{i\sigma}^\dagger$, resp.

- with one-electron integrals h_{ij}

$$h_{ij} = \int \phi_i^*(\mathbf{r}) \left(-\frac{1}{2} \nabla^2 - \sum_I \frac{Z_I}{r_I} \right) \phi_j(\mathbf{r}) d^3r \quad (20)$$

- and two-electron integrals V_{ijkl}

$$V_{ijkl} = \iint \frac{\phi_i^*(\mathbf{r}_1) \phi_j^*(\mathbf{r}_2) \phi_k(\mathbf{r}_2) \phi_l(\mathbf{r}_1)}{r_{12}} d^3r_1 d^3r_2 \quad (21)$$

with spatial molecular orbitals ϕ_i .

Full CI in (Explicit) Second Quantization

- Elementary operators: $a_{i\sigma}^\dagger$ and $a_{i\sigma}$
- Hamiltonian matrix is now constructed from the matrix representation for the elementary operators by direct products
- **By contrast to standard procedure, instead of evaluating the action of the elementary operators on the determinantal basis functions, we set-up a matrix representation of the elementary operators and construct a matrix representation of the Hamiltonian DIRECTLY.**

This Hamiltonian matrix can then be diagonalized.

Elementary operators in (Explicit) Second Quantization

- $a_{i\sigma}^\dagger$ and $a_{i\sigma}$ operate on spin orbital with two states: occ. and unocc.

$$|0\rangle_{i\sigma} = \begin{pmatrix} 1 \\ 0 \end{pmatrix} \quad \text{and} \quad |1\rangle_{i\sigma} = \begin{pmatrix} 0 \\ 1 \end{pmatrix} \quad (22)$$

- Corresponding matrix representation of elementary operators:

$$a_{i\sigma}^\dagger |0\rangle_{i\sigma} = |1\rangle_{i\sigma} \quad \Longleftrightarrow \quad \begin{pmatrix} 0 & 0 \\ 1 & 0 \end{pmatrix} \begin{pmatrix} 1 \\ 0 \end{pmatrix} = \begin{pmatrix} 0 \\ 1 \end{pmatrix} \quad (23)$$

$$a_{i\sigma}^\dagger |1\rangle_{i\sigma} = 0 \quad \Longleftrightarrow \quad \begin{pmatrix} 0 & 0 \\ 1 & 0 \end{pmatrix} \begin{pmatrix} 0 \\ 1 \end{pmatrix} = \begin{pmatrix} 0 \\ 0 \end{pmatrix} \quad (24)$$

$$a_{i\sigma} |0\rangle_{i\sigma} = 0 \quad \Longleftrightarrow \quad \begin{pmatrix} 0 & 1 \\ 0 & 0 \end{pmatrix} \begin{pmatrix} 1 \\ 0 \end{pmatrix} = \begin{pmatrix} 0 \\ 0 \end{pmatrix} \quad (25)$$

$$a_{i\sigma} |1\rangle_{i\sigma} = |0\rangle_{i\sigma} \quad \Longleftrightarrow \quad \begin{pmatrix} 0 & 1 \\ 0 & 0 \end{pmatrix} \begin{pmatrix} 0 \\ 1 \end{pmatrix} = \begin{pmatrix} 1 \\ 0 \end{pmatrix} \quad (26)$$

Matrices for Hamiltonian in (Explicit) Second Quantization

- Dimension of elementary operators defined for orbital space of n spin orbitals with 2 states each: $2^n \Rightarrow$ dimension of the Hamiltonian is 2^n

(NB: for spatial orbitals we have 4^n where 4 is the number of states per orbital [empty, up, down, doubly occupied])

- 2^n -dimensional elementary operator: (the spin index has been omitted for the sake of clarity)

$$a_i^\dagger = \underbrace{\begin{pmatrix} 1 & 0 \\ 0 & -1 \end{pmatrix}_1 \otimes \cdots \otimes \begin{pmatrix} 1 & 0 \\ 0 & -1 \end{pmatrix}_{i-1}}_{\text{matrix structure needed for anticommutation}} \otimes \begin{pmatrix} 0 & 0 \\ 1 & 0 \end{pmatrix}_i \otimes \begin{pmatrix} 1 & 0 \\ 0 & 1 \end{pmatrix}_{i+1} \otimes \cdots \otimes \begin{pmatrix} 1 & 0 \\ 0 & 1 \end{pmatrix}_n$$

matrix structure needed for anticommutation

cf. Jordan–Wigner transformation

- Then, $2^n \times 2^n$ -matrix of term of the one-electron part of Hamiltonian reads:

$$h_{ij} a_i^\dagger a_j = h_{ij} \left[\begin{pmatrix} 1 & 0 \\ 0 & -1 \end{pmatrix}_1 \otimes \cdots \otimes \begin{pmatrix} 1 & 0 \\ 0 & -1 \end{pmatrix}_{i-1} \otimes \begin{pmatrix} 0 & 0 \\ 1 & 0 \end{pmatrix}_i \otimes \begin{pmatrix} 1 & 0 \\ 0 & 1 \end{pmatrix}_{i+1} \otimes \cdots \otimes \begin{pmatrix} 1 & 0 \\ 0 & 1 \end{pmatrix}_n \right] \\ \times \left[\begin{pmatrix} 1 & 0 \\ 0 & -1 \end{pmatrix}_1 \otimes \cdots \otimes \begin{pmatrix} 1 & 0 \\ 0 & -1 \end{pmatrix}_{j-1} \otimes \begin{pmatrix} 0 & 1 \\ 0 & 0 \end{pmatrix}_j \otimes \begin{pmatrix} 1 & 0 \\ 0 & 1 \end{pmatrix}_{j+1} \otimes \cdots \otimes \begin{pmatrix} 1 & 0 \\ 0 & 1 \end{pmatrix}_n \right]$$

- Similar expression for the two-electron part, but product of four 2^n -dimensional elementary matrices

Nothing has been gained yet!

Even worse: Huge matrices have been generated which contain mostly zeros and need to be multiplied and added.

Nothing has been gained yet!

Even worse: Huge matrices have been generated which contain mostly zeros and need to be multiplied and added.

Need to find a way to reduce the dimension !

What is the best reduced many-particle basis?

First attempt: Wilson's renormalization group

Wilson's Renormalization Group: Dimension Reduction

- 1 Choose a number of orbitals l whose many-electron Hamiltonian $H_{el}^{(l)}$ can still be constructed and exactly diagonalized.
- 2 Diagonalize $H_{el}^{(l)}$ of dimension 2^l (or 4^l for spatial orbitals) and select m lowest-energy eigenvectors out of the 2^l eigenvectors.
- 3 Reduce the dimension of $H_{el}^{(l)}$ from 2^l to m by transformation with the rectangular $m \times 2^l$ matrix of eigenvectors.
- 4 Construct $H_{el}^{(l+1)}$ from $H_{el}^{(l)}$ and $H_{el}^{(1)}$ defined for an orbital taken from the $L - l$ remaining orbitals.
- 5 Continue with 2) until $l + 1 = L$.

Issues with Wilson's Renormalization Group

- $H_{el}^{(l)}$ requires exact diagonalization (or a subspace iteration technique like Lanczos, which produces a large portion of the low-energy eigenvectors) and thus its dimension 2^l is limited and l must therefore be rather small
- No guarantee that reduced basis is optimum choice in some sense.
- No information from those $L - l$ remaining orbitals, which have not yet been considered, are taken into account in the construction of $H_{el}^{(l)}$ (particularly bad, when l is small)

What is the best reduced many-particle basis in terms of a least-squares fit?

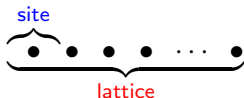
Second attempt: White's DMRG

— transform with eigenvectors of a reduced density matrix

S. R. White, Phys. Rev. Lett. 1992 69 2863; Phys. Rev. B 1993 48 10345

The (two-site) DMRG Algorithm: Terminology

- arrange all **spatial** orbitals as a one-dimensional **lattice**
- lattice consists of **sites**



(27)

- the **sites** of solid state physics are the orbitals in quantum chemistry
- divide lattice into **system block**, two single sites, **environment block**



(active
subsystem)

(explicitly
treated
subsystem)

(complementary
subsystem)

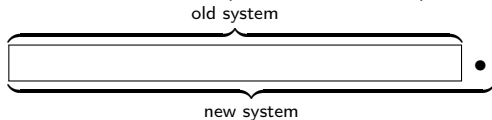
- the joined systems (=CAS) are called the 'superblock'

The DMRG Algorithm: Initialization

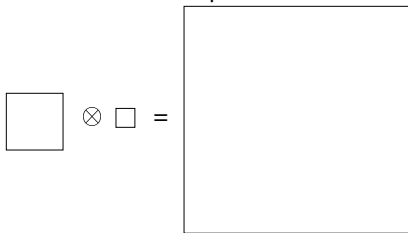
- Construct many-particle states explicitly on active subsystem
- actually: find matrix representation of elementary operators defined on this subsystem
- NB: For a total(!) system of N electrons, many-particle states with 0 to a maximum of N electrons need to be considered
- Hence, active subsystem can comprise only few orbitals (too many sites prohibitive because of factorial scaling of states)
- Find a way to increase the number of orbitals (blocking), while keeping the number of basis states on the active subsystem constant (decimation)

The DMRG Algorithm: Blocking

- enlarge the system (and environment) by one site ('Blocking')



- new states are tensor products of those on old system + those on new site
- calculate operators of new system as direct product of operators defined for old system and new site
- Dimension of operators on old system: m ; Dim. of ops. on single site: 4
 \Rightarrow Dimension of operators defined on new system: $4m$



Construction & Diagonalization of Total Hamiltonian

- consider system and environment each enlarged by one of the explicitly treated sites (dimension for both: $4m$)
- any electronic state defined on the total orbital space (**superblock**) can be written as a tensor product over system $|i\rangle$ and environment $|j\rangle$ basis states

$$\Psi_{el}^{\text{DMRG}} = \sum_{ij} \psi_{ij} |i\rangle \otimes |j\rangle \quad (28)$$

- corresponding **superblock Hamiltonian** $H_{\text{superblock}}$ is calculated as a sum of all elementary operator products defined on enlarged system and enlarged environment (dimension: $4m \times 4m = 16m^2$)
- NB: realize that in the first set of iterations (**sweep**), in which the active subsystem grows orbital by orbital, guessing of a reduced number of states on the environment is required (**warm-up**)
- diagonalize $H_{\text{superblock}}$ to obtain CI-type coefficients ψ_{ij} (scaling: $(16m^2)^3 \approx m^6$ for large $m \rightarrow$ subspace methods: Davidson's diagonalizer)

Construction & Diagonalization of Reduced Density Matrix

- The DMRG CI-type coefficients ψ_{ij} carry two indices as they are explicitly obtained for the i -th system and the j -th environment basis state.
- The reduced density matrix $\rho^{s/e}$ (RDM) for the system can be obtained by tracing out all (sub)states j from the environment:

$$\rho_{ii'}^{s/e} = \sum_{j \in \{e\}} \psi_{ij} \psi_{i'j} \quad (29)$$

- This matrix $\rho_{ii'}^{s/e}$ is of dimension $4m$
- m eigenvectors of $\rho^{s/e}$ can be used for the dimension reduction of all elementary operators from $4m$ back to the original dimension m

Understanding Relation of RDM to Least-Squares Fitting

- We have the following bases at our disposal:
system: $\{|i\rangle; i = 1, \dots, m_s\}$
environment: $\{|j\rangle; j = 1, \dots, m_e\}$
- In the product basis (bipartition) we express a pure state of the superblock (total system; real coefficients assumed):

$$\Psi_{el} = \sum_{ij} \psi_{ij} |i\rangle \otimes |j\rangle \quad (30)$$

- Now search for $m < m_s$ orthogonal, linear-independent system states $\{|u\rangle; u = 1, \dots, m\}$
into which we expand the approximate state

$$\tilde{\Psi}'_{el} = \sum_{uj} c_{uj} |u\rangle \otimes |j\rangle \quad (31)$$

RDM, SVD, and Least-Squares Fitting

- We wish $\Psi_{el} \approx \tilde{\Psi}'_{el}$ by requiring that

$$S' = \left| \Psi_{el} - \tilde{\Psi}'_{el} \right|^2 = \min \quad (32)$$

- Introduce a similar reduced-dimensional basis on the environment:

$\{|v\rangle; v = 1, \dots, m\}$ with $\langle j|v\rangle = c_{vj}$ and $\sum_j |c_{vj}|^2 = 1$
such that the approximate state takes the simple form

$$\tilde{\Psi}_{el} = \sum_k c_k |u_k\rangle \otimes |v_k\rangle \quad (33)$$

(Schmidt decomposition)

- With $U_{ik} = \langle i|u_k\rangle$ and $V_{jk} = \langle j|v_k\rangle$ we have for the squared norm

$$S = \sum_{ij} \left[\psi_{ij} - \sum_k c_k U_{ik} V_{jk} \right]^2 \quad (34)$$

RDM, SVD, and Least-Squares Fitting

- **Here, we recognize the similarity to the least-squares fitting problem in linear algebra!**
- Hence, we may use singular value decomposition (SVD) of a rectangular matrix to minimize $S \rightarrow$ factorize $\psi = (\psi_{ij})$:

$$\psi = U \cdot D \cdot V^T \quad (35)$$

- The matrix $U = (U_{ik})$ is orthogonal and of dimension $m_s \times m_s$.
- The matrix $V = (V_{jk})$ is column-orthogonal and of dimension $m_e \times m_s$.
- D is an m_s -dimensional diagonal matrix and contains the singular values of ψ (assume $m_s \leq m_e$, otherwise consider ψ^T).

RDM, SVD, and Least-Squares Fitting

- The m largest diagonal elements of D are the desired coefficients c_k and the corresponding column vectors of U and V are the desired $|u_k\rangle$ and $|v_k\rangle$.
- **But how can one make the connection to the RDM?**
- Consider the von Neumann density operator for the superblock

$$\hat{\rho} = |\Psi_{el}\rangle\langle\Psi_{el}| \stackrel{(30)}{=} \sum_{ii'jj'} \psi_{ij}\psi_{i'j'}|i\rangle\langle i'| \otimes |j\rangle\langle j'| \quad (36)$$

- reduced density operator from tracing out the environment states

$$\hat{\rho}_s = \text{Tr}_e \hat{\rho} = \sum_{j''} \sum_{ii'jj'} \psi_{ij}\psi_{i'j'}|i\rangle\langle i'| \langle j''|j\rangle\langle j'|j''\rangle \quad (37)$$

$$= \sum_{ii'j} \psi_{ij}\psi_{i'j}|i\rangle\langle i'| \quad (38)$$

RDM, SVD, and Least-Squares Fitting

- The RDM is then obtained as

$$\rho_s = \psi \cdot \psi^T \quad \text{with} \quad (\rho_s)_{ii'} = \sum_j \psi_{ij} \psi_{i'j} \quad (39)$$

- for which we can insert the SVD

$$\rho_s = \psi \cdot \psi^T \stackrel{(35)}{=} (UDV^T) \cdot (VDU^T) = U \cdot D^2 \cdot U^T \quad (40)$$

- Hence, U diagonalizes ρ_s and thus its eigenvalues D_{ii}^2 are related to the coefficients c_k of the Schmidt decomposition !
- Thus, instead of calculating the SVD, one can diagonalize ρ_s to obtain the $c_k = \sqrt{D_{kk}^2}$ from the m highest eigenvalues of D^2 and the corresponding eigenvectors $|u_k\rangle$.
- I.e., the larger the eigenvalue D_{ii}^2 , the better represents $|u_i\rangle$ the system part of the superblock state

RDM, SVD, and Least-Squares Fitting

- Accuracy of approximation can be measured by the truncation error ϵ

$$\epsilon = 1 - \sum_{k=1}^m D_{kk}^2 \quad (41)$$

Ö. Legeza, J. Röder, B. A. Hess, Phys. Rev. B 67 (2003) 125114

- This transfers to the accuracy of an observable O as follows

$$\begin{aligned} |\langle O \rangle_{\Psi_{el}} - \langle O \rangle_{\tilde{\Psi}_{el}}| &= |Tr(O\rho_s) - Tr(O\tilde{\rho}_s)| = \left| \sum_{i=m+1}^{m_s} O_{ii} D_{ii}^2 \right| \\ &\leq \sum_{i=m+1}^{m_s} |O_{ii}| D_{ii}^2 \leq \max_{i>m} |O_{ii}| \sum_{i=m+1}^{m_s} D_{ii}^2 \\ &= \max_{i>m} |O_{ii}| \epsilon \end{aligned} \quad (42)$$

J. Röder, PhD Thesis, University of Erlangen, 2003

Pictorially: Diagonalization of the RDM

- reduced density matrix is diagonalized $\rightarrow 4m$ eigenpairs

$$U = \begin{array}{|c|} \hline 4m \times 4m \\ \hline \end{array}$$

Pictorially: Diagonalization of the RDM

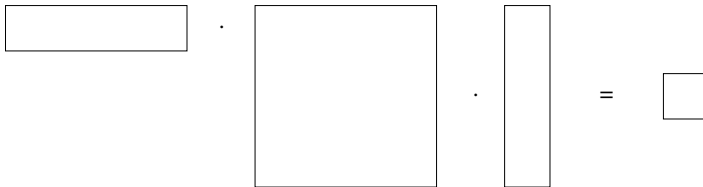
- reduced density matrix is diagonalized $\rightarrow 4m$ eigenpairs

$$U = \begin{array}{|c|} \hline O \\ \hline \end{array}$$

- choose the m eigenvectors with the highest eigenvalues
- keep m variable to always adjust to the optimum number of relevant eigenvectors (Ö. Legeza: dynamic block-state selection DBSS)
- selected eigenvectors transform the many-particle basis of the (enlarged) system to a reduced basis

Pictorially: Renormalization of Operators

- transformation by selected eigenvectors yields new many-particle basis of the system (optimum reduced m -dimensional basis in a least-squares sense)
- operators are now transformed to the new basis, i.e. **renormalized**:


$$\boxed{} \cdot \boxed{\phantom{\tilde{a}_{\text{new}}}} \cdot \boxed{} = \boxed{\phantom{a_{\text{new}}}}$$

$$O^T \tilde{a}_{\text{new}} O = a_{\text{new}} \quad (43)$$

- columns of the transformation matrix O consist of the selected eigenvectors
- dimension of the operators is reduced from $4m$ to m

Features of the DMRG Algorithm

- DMRG is a CAS approach!
- DMRG iterations increase AS orbital by orbital until the environment is completely absorbed into the system.
- Then, the iteration direction is reversed to optimize the environment representation.
- This defines a 'linear' algorithm, and explains why the orbital ordering can be important (convergence to local minima possible!).

G. Moritz, B. A. Hess, M. Reiher, *J. Chem. Phys.* **2005** 122 024107

- It was thought that DMRG is therefore only beneficial for pseudo-one-dimensional molecules.
- DMRG state is a superposition of FCI-type basis states.
- An FCI/CAS solution can be converged; but the basis cannot be completely known in terms of CSFs if DMRG shall be efficient

DMRG Convergence for Complicated Electronic Structures

- If DMRG calculations shall be competitive, these issues must be addressed:
 - **dynamic correlation effects need to be included**
see work of G. K.-L. Chan *et al.*, T. Yanai & Y. Kurashige *et al.* on multi-reference perturbation theory;
problem: requires up to 4-body reduced density matrices !
 - **efficient warm-up sweep (environment guess)**
see work of Ö. Legeza *et al.* (CI-DEAS and entanglement measures for orbital ordering)
 - **number of renormalized states m should be as small as possible**
- **orbital ordering:**
crucial to avoid convergence to local energy minima in case of small m
(if no noise or perturbative correction are considered)
G. Moritz, B. A. Hess, M. Reiher, *J. Chem. Phys.* **2005** 122 024107
- **environment states:** in principle, the better the approximation of environment states the faster convergence should be
G. Moritz, M. Reiher, *J. Chem. Phys.* **2006** 124 034103

Determining Factors of DMRG Convergence

- ① (Choice of the one-electron basis set for the representation of the molecular orbitals)
- ② Size of the active space (CAS)
- ③ Choice of the type of molecular orbitals (HF, NO's, localized orbitals, ..., DMRG-SCF)
- ④ Environment-state guess in the first sweep (CI-DEAS by Ö. Legeza or noise/perturbation added to RDM)
- ⑤ Ordering of orbitals (exploit entanglement measures, see below)
- ⑥ Number of renormalized subsystem states m

⇒ **All of these parameters must be documented in a report on DMRG results !**

Lecture 2

Second-Generation DMRG: Matrix Product and Tensor Network States

- 1 New Parametrization of the Electronic Wave Function: Tensor Network States (TNS)
- 2 Matrix Product States (MPSs) and Matrix Product Operators (MPOs)
- 3 Parameters that Determine DMRG Accuracy

How to Efficiently Represent (Electronic) Quantum States?

- Tensor-product construction of the N -particle Hilbert space from 1-particle Hilbert spaces

$$\Psi_{el} = \sum_{i_1 i_2 \dots i_L} C_{i_1 i_2 \dots i_L} |i_1\rangle \otimes |i_2\rangle \otimes \dots \otimes |i_L\rangle \quad (44)$$

- Dimension increases exponentially with system size (4^L for spatial orbitals). $C_{i_1 i_2 \dots i_L}$ ($=C_I$) is element of the coefficient tensor
- In principle, it should be sufficient to parameterize a manifold of states such that there exists a large overlap with the exact state.

F. Verstraete, *Adv. Phys.* **2008** 57 143

- How to **reduce the complexity of Ψ_{el}** and come up with a class of variational wave functions that captures the physics of the electronic Hamiltonian?

Parameterization of the Wave Function

$$\Psi_{el} = \sum_{i_1 i_2 \dots i_L} C_{i_1 i_2 \dots i_L} |i_1\rangle \otimes |i_2\rangle \otimes \dots \otimes |i_L\rangle \quad (45)$$

- Configuration Interaction ansatz

$$|\text{CI}\rangle = \left(1 + \sum_{\mu} C_{\mu} \hat{\tau}_{\mu}\right) |\text{HF}\rangle \quad (46)$$

- Coupled Cluster ansatz

$$|\text{CC}\rangle = \left(\prod_{\mu} [1 + t_{\mu} \hat{\tau}_{\mu}]\right) |\text{HF}\rangle \quad (47)$$

- Restricted sum over basis states with a certain substitution pattern generated by 'excitation' operator $\hat{\tau}_{\mu}$
→ yields a pre-defined (!) many-particle basis set
- numerous specialized selection/restriction protocols

Instead of standard CI-type calculations by diagonalization/projection

$$\Psi_{el} = \sum_{i_1 i_2 \dots i_L} C_{i_1 i_2 \dots i_L} |i_1\rangle \otimes |i_2\rangle \otimes \dots \otimes |i_L\rangle \quad (48)$$

construct CI coefficients from correlations among orbitals

$$\Psi_{el} = \sum_{i_1 i_2 \dots i_L} C_{i_1 i_2 \dots i_L} |i_1\rangle \otimes |i_2\rangle \otimes \dots \otimes |i_L\rangle \quad (49)$$

\Rightarrow tensor construction of expansion coefficients

Some Early Tensor Network (TN) Approaches

... for spin Hamiltonians developed:

- 1-dimensional TN: **Matrix Product States** (MPS) / DMRG

S. R. White, *Phys. Rev. Lett.* **1992** 69 2863

S. Römmer, S. Ostlund, *Phys. Rev. Lett.* **1995** 75 3537

- 2-dimensional TN: **Projected Entangled Pair States** (PEPS)

F. Verstraete, M. M. Wolf, D. Perez-Garcia, J. I. Cirac *PRL* **2006** 96 220601

- higher-dimensional TN:

Multiscale Entanglement Renormalization Ansatz (MERA)

M. Aguado, G. Vidal, *Phys. Chem. Rev.* **2008** 100 070404

MPS & DMRG

- Structure of White's DMRG wave function: Matrix Product States (MPS)

S. Römmer, S. Ostlund, *Phys. Rev. Lett.* **1995** 75 3537

$$\Psi_{el}^{\text{MPS}} = \sum_{i_1 i_2 \dots i_L} \left[A_{i_1}^{[1]} \cdots A_{i_L}^{[L]} \right] |i_1 \otimes i_2 \otimes \cdots \otimes i_L\rangle \quad (50)$$

- **DMRG algorithm defines a protocol for the iterative improvement of the matrices $A^{[i]}$ by using the reduced density matrix (RDM) for the AS of the total system.**
- Transformation matrices $A^{[i]}$ represent the change of the many-electron basis when adding to the *active subsystem* (AS) states on a single orbital taken from the *environment*.
- In the finite-CAS DMRG, the first and last matrices $A_{i_1}^{[1]}$ and $A_{i_L}^{[L]}$, resp., are actually vectors.

Reconstruction of CI coefficients

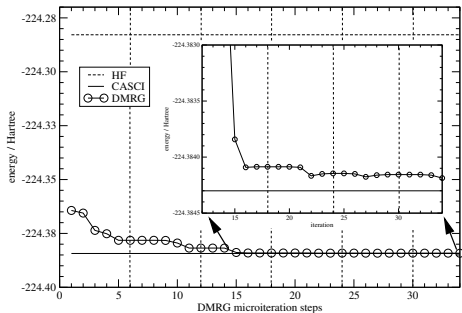
- **Reconstruct a CI-type wave function from the DMRG state, because**
 - allows us to interpret/understand the states in the standard way,
 - makes DMRG calculations for different m values comparable,
 - allows us to study DMRG convergence in terms of determinants being picked up.
- MPS structure yields the CI coefficients:

$$C_{\{\mathbf{n}\}} = \sum_{m_s}^m \sum_{m_e}^m \psi_{m_s n_{l+1} n_{l+2} m_e} \left(A_l^{[n_l]} \dots A_2^{[n_2]} \right)_{m_s; n_1} \times \left(A_{l+3}^{[n_{l+3}]} \dots A_{L-1}^{[n_{L-1}]} \right)_{m_e; n_L} \quad (51)$$

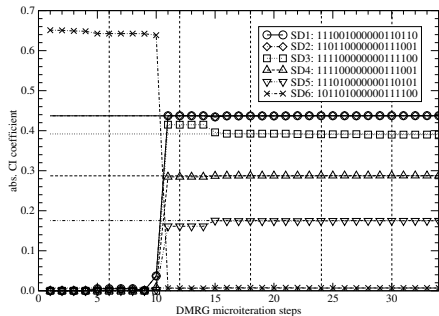
CI coefficient calculated from renormalization matrices and DMRG-state expansion coefficients $\psi_{m_s n_{l+1} n_{l+2} m_e}$ (for active system of size l)

Example: Transition Structure of Ozone

O₃ transition state energy



O₃ transition state CI coefficients

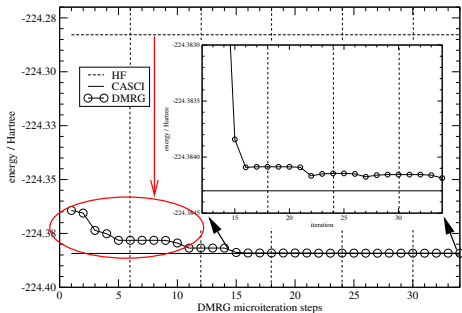


G. Moritz, M. Reiher, *J. Chem. Phys.* 126 (2007) 244109

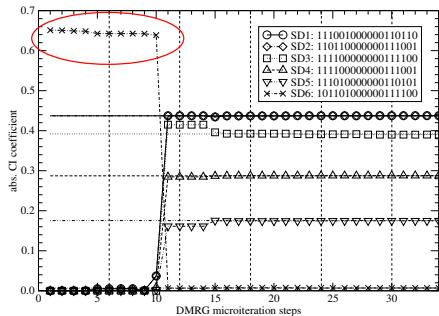
(see this reference also for a DMRG flow chart)

Example: Transition Structure of Ozone

O₃ transition state energy



O₃ transition state CI coefficients

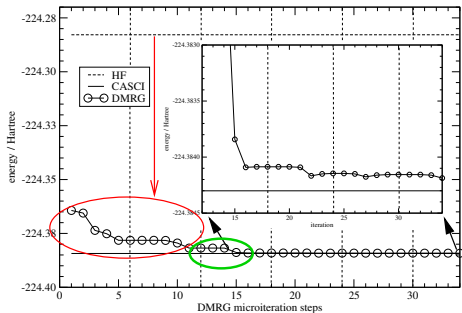


G. Moritz, M. Reiher, *J. Chem. Phys.* 126 (2007) 244109

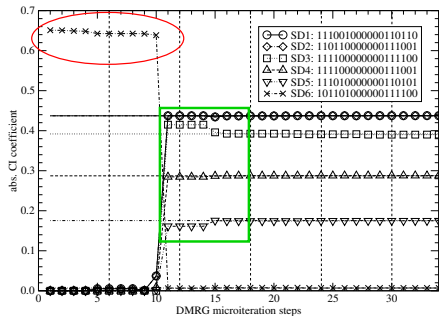
(see this reference also for a DMRG flow chart)

Example: Transition Structure of Ozone

O₃ transition state energy



O₃ transition state CI coefficients



G. Moritz, M. Reiher, *J. Chem. Phys.* 126 (2007) 244109

(see this reference also for a DMRG flow chart)

SR-CAS Approach

- Our 2007 scheme could only reconstruct FCI from DMRG wave functions for which a FCI calculation was also possible.
- Cure: Sampling-Reconstruction Complete-Active-Space algorithm:
Monte Carlo scheme for sampling configurations
- Only the most important configurations are kept.
- The accuracy is easily controlled by a completeness measure COM:

$$\text{COM} = 1 - \sum_{I \in \{\text{sample}\}} C_I^2 \quad (52)$$

K. Boguslawski, K. H. Marti, M. Reiher, *J. Chem. Phys.* 134 (2011) 224101

Derivation of MPS Structure of DMRG Wave Function

The CI coefficient tensor $C_{i_1 i_2 \dots i_L}$

$$\begin{aligned}\Psi_{el} &= \sum_{i_1 i_2 \dots i_L} C_{i_1 i_2 \dots i_L} |i_1\rangle \otimes |i_2\rangle \otimes \dots \otimes |i_L\rangle \\ &\equiv \sum_{i_1 i_2 \dots i_L} C_{i_1 i_2 \dots i_L} |i_1, i_2, \dots, i_L\rangle \equiv \sum_I C_I \Phi_I\end{aligned}\quad (53)$$

can be decomposed by sequential SVDs, which clarifies the MPS structure of the DMRG wave function.

Consider a DMRG state function with the first orbital (from the left) in the AS and $(L - 1)$ orbitals in the environment,

$$\Psi_{el}^{\text{DMRG}} = \sum_{i_1 \mathbf{j}} \psi_{i_1 \mathbf{j}} |i_1\rangle \otimes |\mathbf{j}\rangle \quad \text{with } \mathbf{j} = (i_2 \dots i_L) \quad (54)$$

Hence, the coefficient tensor $C_{i_1 i_2 \dots i_L}$ is approximated by a matrix $\psi_{i_1 \mathbf{j}}$.

Derivation of MPS Structure of DMRG Wave Function

$\psi_{i_1 \mathbf{j}}$ is of dimension $(m \times m^{L-1})$ and can be subjected to an SVD

$$\begin{aligned} C_{i_1 i_2 \dots i_L} \rightarrow \psi_{i_1 \mathbf{j}} = \psi_{i_1 (i_2 \dots i_L)} &= \sum_{a_1}^{r_1} U_{i_1 a_1} D_{a_1 a_1} V_{a_1 (i_2 \dots i_L)}^T \\ &\equiv \sum_{a_1}^{r_1} U_{i_1 a_1} C_{a_1 i_2 \dots i_L} \end{aligned} \quad (55)$$

with the rank $r_1 \leq m$. Now, change notation:

a) matrix U is written as a collection of row vectors A^{i_1} with entries

$$A_{a_1}^{i_1} = U_{i_1 a_1}.$$

b) coefficient tensor $C_{a_1 i_2 \dots i_L}$ is ordered as a matrix $\psi_{(a_1 i_2)(i_3 \dots i_L)}$ of dimension $(r_1 \cdot m \times m^{L-2})$

Derivation of MPS Structure of DMRG Wave Function

... so that we obtain for the original coefficient tensor

$$C_{i_1 i_2 \dots i_L} = \sum_{a_1}^{r_1} A_{a_1}^{i_1} \psi_{(a_1 i_2)(i_3 \dots i_L)} \quad (56)$$

Next, the matrix $\psi_{(a_1 i_2)(i_3 \dots i_L)}$ is subjected to another SVD

$$\psi_{(a_1 i_2)(i_3 \dots i_L)} = \sum_{a_2}^{r_2} U_{(a_1 i_2) a_2} D_{a_2 a_2} V_{a_2 (i_3 \dots i_L)}^T \quad (57)$$

$$\equiv \sum_{a_2}^{r_2} U_{(a_1 i_2) a_2} C_{a_2 i_3 \dots i_L} \quad (58)$$

$$\equiv \sum_{a_2}^{r_2} A_{a_1 a_2}^{i_2} \psi_{(a_2 i_3)(i_4 \dots i_L)} \quad (59)$$

where the last step is again just a change of notation ...

Derivation of MPS Structure of DMRG Wave Function

... which, however, allows us to write the original tensor in compact form

$$C_{i_1 i_2 \dots i_L} = \sum_{a_1}^{r_1} \sum_{a_2}^{r_2} A_{a_1}^{i_1} A_{a_1 a_2}^{i_2} \psi_{(a_2 i_3)(i_4 \dots i_L)} \quad (60)$$

Now, the new matrix $\psi_{(a_2 i_3)(i_4 \dots i_L)}$ of dimension $(r_2 \cdot m \times m^{L-3})$ is subjected to the next SVD.

This 'game' continues until we finally obtain

$$C_{i_1 i_2 \dots i_L} = \sum_{a_1 \dots a_L} A_{a_1}^{i_1} A_{a_1 a_2}^{i_2} \dots A_{a_{L-2} a_{L-1}}^{i_{L-1}} A_{a_{L-1}}^{i_L} \quad (61)$$

$$= A^{i_1} A^{i_2} \dots A^{i_{L-1}} A^{i_L} \quad (62)$$

where the sums are interpreted as matrix multiplications in the last step.

MPS Structure of Operators: MPOs

Consider occupation-number-vector basis states $|\sigma\rangle$ and $|\sigma'\rangle$.

The coefficients $w_{\sigma\sigma'}$ of a general operator

$$\widehat{\mathcal{W}} = \sum_{\sigma, \sigma'} w_{\sigma\sigma'} |\sigma\rangle \langle \sigma'|, \quad (63)$$

may be encoded in matrix-product form

$$w_{\sigma, \sigma'} = \sum_{i_1, \dots, i_{L-1}} W_{1i_1}^{\sigma_1 \sigma'_1} \cdots W_{i_{l-1} i_l}^{\sigma_l \sigma'_l} \cdots W_{i_{L-1} 1}^{\sigma_L \sigma'_L}. \quad (64)$$

Combining Eqs. (63) and (64), operator $\widehat{\mathcal{W}}$ reads

$$\widehat{\mathcal{W}} = \sum_{\sigma, \sigma'} \sum_{i_1, \dots, i_{L-1}} W_{1i_1}^{\sigma_1 \sigma'_1} \cdots W_{i_{l-1} i_l}^{\sigma_l \sigma'_l} \cdots W_{i_{L-1} 1}^{\sigma_L \sigma'_L} |\sigma\rangle \langle \sigma'|. \quad (65)$$

Simplify Eq. (65) by contraction over the local site indices σ_l, σ'_l in σ, σ' :

$$\widehat{W}_{i_{l-1}i_l}^l = \sum_{\sigma_l, \sigma'_l} W_{i_{l-1}i_l}^{\sigma_l \sigma'_l} |\sigma_l\rangle \langle \sigma'_l|, \quad (66)$$

so that Eq. (65) reads

$$\widehat{\mathcal{W}} = \sum_{i_1, \dots, i_{L-1}} \widehat{W}_{1i_1}^1 \cdots \widehat{W}_{i_{l-1}i_l}^l \cdots \widehat{W}_{i_{L-1}1}^L. \quad (67)$$

Motivation for this: Entries of the resulting $\widehat{W}_{i_{l-1}i_l}^l$ matrices are the elementary operators $\hat{a}_{l\sigma}^\dagger$ and $\hat{a}_{l\sigma}$ acting on a single site (=orbital)!

MPS concept has thus been transferred to operators (MPOs).

A program that implements these equations, we call a second-generation DMRG program.

Why write a new code? – Two variants of DMRG:

Traditional DMRG

- $|\psi\rangle = \sum_{LR} C_{LR} |\sigma_L\rangle \otimes |\sigma_R\rangle$
- coefficients valid for one bipartition into L and R (need basis transformations)
- considered to be faster for ground state

MPO-DMRG

- $|\psi\rangle = \sum_{\sigma} M^{\sigma_1} M^{\sigma_2} \dots M^{\sigma_L} |\sigma\rangle$
- coefficients valid for whole system
- Easy and efficient implementation of observables
- QC-MAQUIS developed in my group by S. Keller, S. Knecht, Y. Ma, C. Stein, S. Battaglia, E. Hedegard is based on the MPO-based DMRG program MAQUIS by Troyer and co-workers for spin Hamiltonians

Other Options: Tensor Network States (TNS)

$$\Psi_{el}^{\text{TNS}} = \sum_{i_1 i_2 \dots i_L} \prod_i^L \prod_{j \leq i} f_{ij}^{I[i]I[j]} \underbrace{|i_1\rangle \otimes |i_2\rangle \otimes \dots \otimes |i_L\rangle}_{|I\rangle} \quad (68)$$

- Idea: Rewrite CI coefficient tensor by reducing number of variational parameters (still obtain qualitatively correct wave function).

- **TNS originally proposed for simple *Spin Hamiltonians*:**

- String-Bond States

N. Schuch, M. Wolf, F. Verstraete, J. I. Cirac, *Phys. Rev. Lett.* **2008** 100 040501

- Entangled-Plaquette States

F. Mezzacapo, N. Schuch, M. Boninsegni, J. I. Cirac **2009** arXiv:0905.3898v3

- Correlator-Product States

H. J. Changlani, J. M. Kinder, C. J. Umrigar, G. K.-L. Chan, **2009** arXiv:0907.4646v1

Complete-Graph Tensor Network States (CG-TNS)

- First implementation of TNS for full quantum-chemical Hamiltonian
- Considering *all* pairs of parameters f_{ij} : CG-TNS
- Parameters optimized with Monte Carlo techniques
- First studied for methylene and ozone; S/T splitting in ozone:

| | $E_{S=0}/E_h$ | $E_{S=1}/E_h$ | $\Delta E/\text{kcalmol}^{-1}$ |
|--------|---------------|---------------|--------------------------------|
| HF | -224.282 841 | -224.357 167 | 46.6 |
| CASCI | -224.384 301 | -224.416 172 | 20.0 |
| CG-TNS | -224.381 648 | -224.412 775 | 19.5 |

K. H. Marti, B. Bauer, M. Reiher, M. Troyer, F. Verstraete, *New J. Phys.* **12** 2010 103008

Variational Quantum Monte Carlo

$$\Psi_{el}^{TNS} = \sum_{i_1 i_2 \dots i_N} \prod_i \prod_{j \leq i}^N f_{ij}^{I[i]I[j]} \underbrace{|I\rangle}_{|i_1 i_2 \dots i_N\rangle} = \sum_I W(I) |I\rangle$$

$$E = \langle E(I) \rangle = \frac{1}{Z} \sum_I W^2(I) E(I) \quad \text{where} \quad Z = \sum_I W^2(I)$$

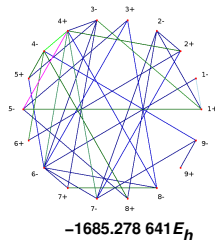
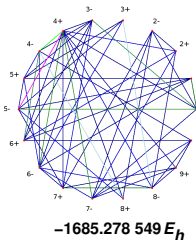
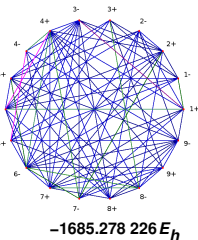
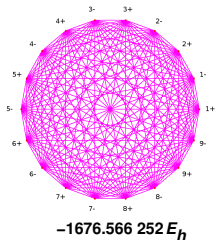
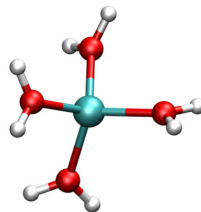
$$E(I) = \sum_{I'} \frac{W(I')}{W(I)} \langle I' | H | I \rangle$$

- The energy can be evaluated using importance sampling of the configurations $|I\rangle$ according to the weight $W^2(I)$.

A. W. Sandvik, G. Vidal, *Phys. Rev. Lett.* **2007** 99 220602

CG-TNS for Transition Metal Compounds

- CG-TNS will be efficient if the molecular structure supports the ansatz (clusters!)
- Problem: One must avoid the explicit construction of all CSFs
- First feasibility test: tetraqua-cobalt
K. H. Marti, M. Reiher, *PCCP* 13 (2011) 6750



| | Hartree-Fock | CAS(9,9)-SCF | CG-TNS |
|--------------------|---------------|---------------|---------------|
| E_{el} / Hartree | -1685.235 055 | -1685.293 744 | -1685.279 408 |
| Var. Parameters | | 7056 | 684 |

Applications

Results of Actual Quantum-Chemical Calculations

(taken from our group)

- 1 DMRG for Compact Strongly Correlated Molecules:
Transition Metal Complexes
- 2 DMRG Spin Density
- 3 Concepts of Quantum Information Theory for Electronic Structures
and Chemical Bonding

Does DMRG Work for Compact Molecules?

- Original 'opinion' in the DMRG community:

Works only for pseudo-one-dimensional, non-compact systems!

- Test for a mononuclear transition metal system CAS(10,10): **CoH**

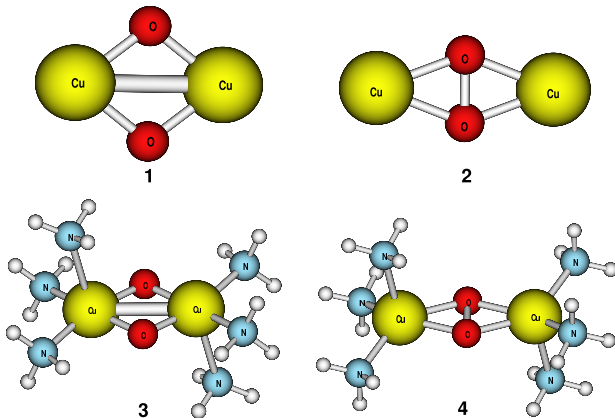
| m | E_{singlet}/E_h | E_{triplet}/E_h | $\Delta E/\text{kJmol}^{-1}$ |
|---------------|--------------------------|--------------------------|------------------------------|
| 64 | -1381.952 054 | -1381.995 106 | 113.03 |
| 76 | -1381.952 063 | -1381.995 109 | 113.02 |
| 91 | -1381.952 070 | -1381.995 110 | 113.00 |
| 109 | -1381.952 073 | -1381.995 110 | 112.99 |
| CAS(10,10) | -1381.952 074 | -1381.995 110 | 112.99 |
| CASPT2(10,10) | -1382.189 527 | -1382.241 333 | 130.57 |
| DFT/BP86 | -1383.504 019 | -1383.585 212 | 213.1 |
| DFT/B3LYP | -1383.202 267 | -1383.279 574 | 203.0 |

original work to propose DMRG for compact, strongly correlated molecules:

K. Marti, I. Malkin Ondik, G. Moritz, M. Reiher, *J. Chem. Phys* 128 (2008) 014104

The Cu_2O_2 -Torture Track

- Standard CASSCF fails for large CASs relevant in polynuclear clusters
- Example: two different isomers of dinuclear copper clusters



C. J. Cramer, M. Włoch, P. Piecuch, C. Puzzarini, L. Gagliardi *J. Phys. Chem. A* 110 (2006) 1991

Energies of Isomeric Dinuclear Copper Clusters

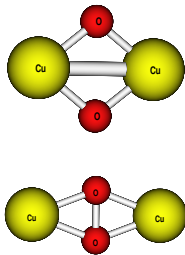
- CASSCF fails since large CASs needed for clusters

K. Marti, I. Malkin Ondik, G. Moritz, M. Reiher, *JCP* 128 (2008) 014104

- results with new code and including noise:

44 active orbitals, 26 electrons, basis set: Cu ECP10MDF, O ANO-Sm, charge: +2

K. Marti, M. Reiher, *Z. Phys. Chem.* 224 (2010) 583



| m | E_{bisoxo}/E_h | E_{peroxo}/E_h | $\Delta E/\text{kJmol}^{-1}$ |
|----------------------------|-------------------------|-------------------------|------------------------------|
| DMRG($m=32$) | -541.440 272 | -541.478 196 | 99.6 |
| DMRG($m=44$) | -541.446 006 | -541.483 405 | 98.2 |
| DMRG($m=64$) | -541.458 021 | -541.497 468 | 103.6 |
| DMRG($m=128$) | -541.473 082 | -541.514 702 | 109.3 |
| RASPT2(24,28) ^a | | | 119.66 |

^aP. Å. Malmqvist, et al. *J. Chem. Phys* 128 (2008) 204109

- What is the fully converged DMRG result for this system?

→ Large-scale DMRG: 149 kJ/mol Y. Kurashige, T. Yanai, *J. Chem. Phys.* 130 (2009) 234114 ... Final answer ?

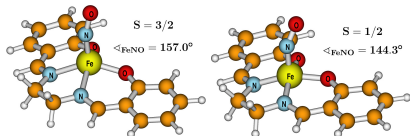
Torture Track: $[\text{Cu}_2\text{O}_2]^{2+}$

| Ref.,method | E_{bisoxo} | E_{peroxo} | ΔE |
|---|---------------------|---------------------|------------|
| 'Standard' methods | | | |
| A),CASSCF(16,14) | −541.50307 | −541.50345 | 1 |
| A),CASPT2(16,14) | −542.06208 | −542.06435 | 6 |
| A),bs-B3LYP | −544.19419 | −544.27844 | 221 |
| B),RASPT2(24,28) | | | 120 |
| Previously published DMRG energies | | | |
| C),DMRG(26,44)[800] | −541.46779 | −541.49731 | 78 |
| D),DMRG(26,44)[128] | −541.47308 | −541.51470 | 109 |
| E),DMRG(32,62)[2400] | −541.96839 | −542.02514 | 149 |
| F),DMRG(28,32)[2048]-SCF | −541.76659 | −541.80719 | 107 |
| F),DMRG(28,32)[2048]-SCF/CT | | | 113 |
| our latest DMRG results with QIT, without noise | | | |
| G), DMRG(26,44)[256/1024/10 ^{−5}] | −541.53853 | −541.58114 | 112 |

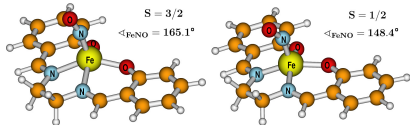
A) C. J. Cramer *et al.*, *J. Phys. Chem. A* 110 (2006) 1991; B) P. A. Malmqvist *et al.*, *J. Chem. Phys* 128 (2008) 204109; C) K. Marti, *et al.*, *J. Chem. Phys* 128 (2008) 014104; D) K. Marti, M. Reiher, *Z. Phys. Chem.* 224 (2010) 583; E) Y. Kurashige, T. Yanai, *J. Chem. Phys.* 130 (2009) 234114; F) T. Yanai *et al.*, *J. Chem. Phys.* 132 (2010) 024105; G) G. Barcza *et al.*, *Phys. Rev. A* 83 (2011) 012508

Analysis of Spin Density Distributions with DMRG

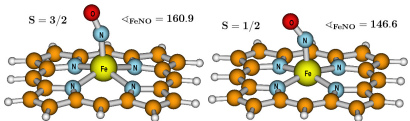
Example 4: Noninnocent Iron Nitrosyl Complexes



(a) Fe(salen)(NO) conformation a



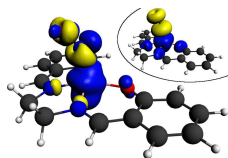
(b) Fe(salen)(NO) conformation b



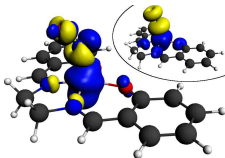
(c) Fe(porphyrin)(NO)

- transition metal nitrosyl complexes have a complicated electronic structure
- qualitatively different spin densities reported by Conradie & Ghosh
J. Conradie, A. Ghosh, J. Phys. Chem. B **2007**, *111*, 12621.
- systematic comparison of DFT spin densities with CASSCF:
K. Boguslawski, C. R. Jacob, M. Reiher, J. Chem. Theory Comput. **2011**, *7*, 2740;
see also work by K. Pierloot *et al.*

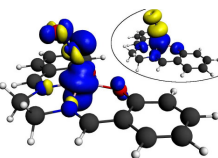
DFT Spin Densities: A Case Study



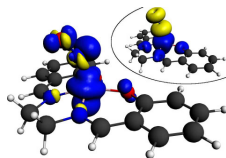
(a) OLYP



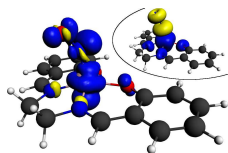
(b) OPBE



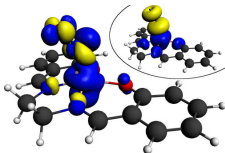
(c) BP86



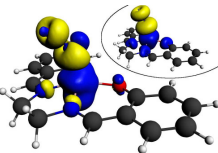
(d) BLYP



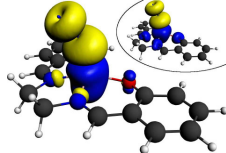
(e) TPSS



(f) TPSSH



(g) M06-L

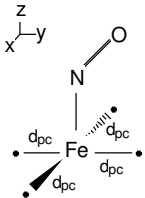


(h) B3LYP

- Only for high-spin complexes similar spin densities are obtained

⇒ $[\text{Fe}(\text{NO})]^{2+}$ moiety determines the spin density

The Model System for Accurate Reference Calculations



Structure:

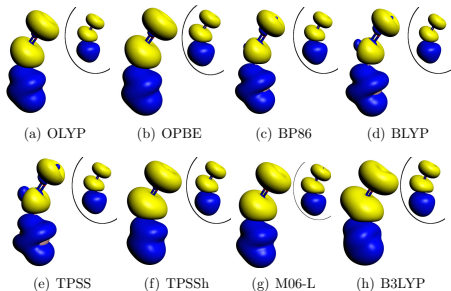
- Four point charges of -0.5 e model a square-planar ligand field ($d_{dp} = 1.131\text{ \AA}$)
- ⇒ Similar differences in DFT spin densities as present for larger iron nitrosyl complexes

Advantage of the small system size:

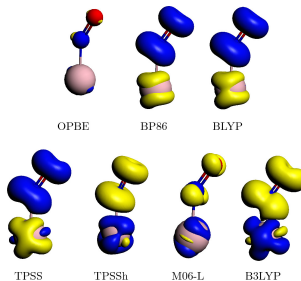
- Standard correlation methods (CASSCF, ...) can be efficiently employed
- Study convergence of the spin density w.r.t. the size of the active orbital space

K. Boguslawski, C. R. Jacob, M. Reiher, *J. Chem. Theory Comput.* **2011**, 7, 2740.

DFT Spin Densities



Spin density isosurface plots



Spin density difference plots w.r.t.
OLYP

⇒ Similar differences as found for the large iron nitrosyl complexes

Reference Spin Densities from Standard Electron Correlation Methods

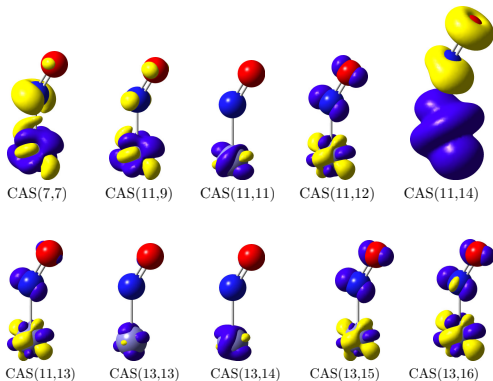
Reference Spin Densities from CASSCF Calculations

Defining the active orbital space:

- Minimal active space: Fe $3d$ - and both NO π^* -orbitals \Rightarrow **CAS(7,7)**
- Consider also both NO π -orbitals \Rightarrow **CAS(11,9)**
- Additional shell of Fe d -orbitals (double-shell orbitals) is gradually included \Rightarrow **CAS(11,11)** to **CAS(11,14)**
- Include one ligand σ -orbital and the antibonding σ^* -orbital upon the CAS(11,11) \Rightarrow **CAS(13,13)**

\Rightarrow Analyze convergence of spin density w.r.t. the dimension of the active orbital space

CASSCF Results: Oscillating Spin Densities



- CAS(11,14): spin density; all others: spin density differences
- stable CAS with all important orbitals is difficult to obtain

⇒ Reference spin densities for very large CAS required

The Non-Relativistic DMRG Spin Density

Calculation of DMRG spin density requires expression in 2nd quantization

$$Q(\mathbf{r}) = \frac{1}{2} \sum_{pq} \phi_p^*(\mathbf{r}) \phi_q(\mathbf{r}) \langle \Psi | a_{p\alpha}^\dagger a_{q\alpha} - a_{p\beta}^\dagger a_{q\beta} | \Psi \rangle \quad (69)$$

Recall:

- The DMRG lattice with natural orbitals $\{\phi_i(\mathbf{r})\}$ as lattice sites



- Operator expression for a_1 and a_2 defined on $\tilde{\mathcal{F}} = \tilde{\mathcal{F}}_1 \otimes \tilde{\mathcal{F}}_2 \otimes \tilde{\mathcal{F}}_3$:

$$a_1^{\tilde{\mathcal{F}}} : a_1 \otimes \mathbf{1}_{\tilde{\mathcal{F}}_2} \otimes \mathbf{1}_{\tilde{\mathcal{F}}_3} \quad (70)$$

$$a_2^{\tilde{\mathcal{F}}} : \mathbf{A}_{\tilde{\mathcal{F}}_1} \otimes a_2 \otimes \mathbf{1}_{\tilde{\mathcal{F}}_3} \quad (71)$$

DMRG Spin Densities — Measures of Convergence

- **Qualitative** convergence measure: spin density difference plots
- **Quantitative** convergence measure:

$$\Delta_{\text{abs}} = \int |\rho_1^{\text{s}}(\mathbf{r}) - \rho_2^{\text{s}}(\mathbf{r})| d\mathbf{r} < 0.005 \quad (72)$$

$$\Delta_{\text{sq}} = \sqrt{\int |\rho_1^{\text{s}}(\mathbf{r}) - \rho_2^{\text{s}}(\mathbf{r})|^2 d\mathbf{r}} < 0.001 \quad (73)$$

- **Quantitative** convergence measure: quantum fidelity F_{m_1, m_2}

$$F_{m_1, m_2} = |\langle \Psi^{(m_1)} | \Psi^{(m_2)} \rangle|^2 \quad (74)$$

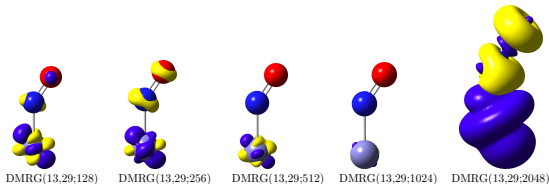
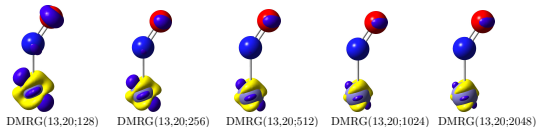
⇒ Reconstructed CI expansion of DMRG wave function can be used!

K. Boguslawski, K. H. Marti, M. Reiher, *J. Chem. Phys.* **2011**, *134*, 224101.

DMRG Spin Densities for Large Active Spaces

Δ_{abs} and Δ_{sq} for DMRG(13, y)[m] calculations w.r.t. DMRG(13,29)[2048] reference

| Method | Δ_{abs} | Δ_{sq} | Method | Δ_{abs} | Δ_{sq} |
|-------------------|-----------------------|----------------------|-------------------|-----------------------|----------------------|
| DMRG(13,20)[128] | 0.030642 | 0.008660 | DMRG(13,29)[128] | 0.032171 | 0.010677 |
| DMRG(13,20)[256] | 0.020088 | 0.004930 | DMRG(13,29)[256] | 0.026005 | 0.006790 |
| DMRG(13,20)[512] | 0.016415 | 0.003564 | DMRG(13,29)[512] | 0.010826 | 0.003406 |
| DMRG(13,20)[1024] | 0.015028 | 0.003162 | DMRG(13,29)[1024] | 0.003381 | 0.000975 |
| DMRG(13,20)[2048] | 0.014528 | 0.003028 | | | |

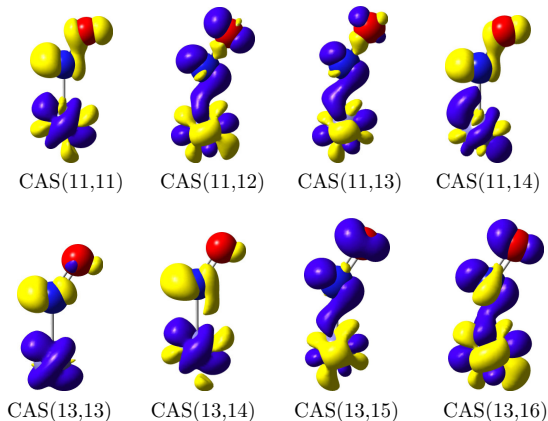


Importance of Empty Ligand Orbitals

Table : Some important Slater determinants with large CI weights from DMRG(13,29)[m]
 Upper part: Slater determinants containing an occupied $d_{x^2-y^2}$ -double-shell orbital (marked in bold face). Bottom part: Configurations with occupied ligand orbitals (marked in bold face). 2: doubly occupied; a: α -electron; b: β -electron; 0: empty.

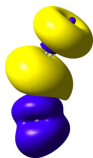
| Slater determinant | CI weight | |
|---|------------|------------|
| | $m = 128$ | $m = 1024$ |
| b2b222a0a0000000 0000000 a 00000 | 0.003 252 | 0.003 991 |
| bb2222aa00000000 0000000 a 00000 | -0.003 226 | -0.003 611 |
| 222220ab00000000 0000000 a 00000 | -0.002 762 | -0.003 328 |
| ba2222ab00000000 0000000 a 00000 | 0.002 573 | 0.003 022 |
| b2a222a0b0000000 0000000 a 00000 | -0.002 487 | -0.003 017 |
| 202222ab00000000 0000000 a 00000 | 0.002 405 | 0.002 716 |
| b222a2a0b0000000 0000000 0 0000a | 0.010 360 | 0.011 558 |
| 22b2a2a0a0000000 0000000 0 b0000 | 0.009 849 | 0.011 366 |
| 22b2a2a0b0000000 0000000 0 a0000 | -0.009 532 | -0.011 457 |
| b2222aab00000000 0000000 0 0000a | -0.009 490 | -0.010 991 |
| a2222baa00000000 0000000 0 0000b | -0.009 014 | -0.010 017 |
| b2b222a0a0000000 0000000 0 0a000 | 0.008 820 | 0.010 327 |

Assessment of CASSCF Spin Densities (Differences)

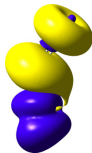


⇒ CASSCF spin densities oscillate around DMRG reference distribution

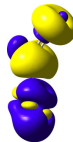
DFT-DMRG Spin Densities Differences



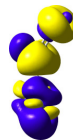
OLYP



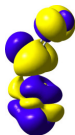
OPBE



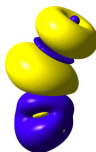
BP86



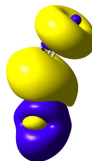
BLYP



TPSS



TPSSH



M06-L



B3LYP

K. Boguslawski, K. H. Marti, Ö. Legeza, M. Reiher, *J. Chem. Theory Comput.* **8** 2012 1970

Analyzing DMRG and correlated wave functions with concepts from quantum information theory

Entanglement Measures for Embedded Subsystems

- see pioneering work by Ö. Legeza !
- Consider one or two orbitals embedded in a CAS
- Measure for the entanglement of orbital i with the environment:
Ö. Legeza, J. Sólyom, *Phys. Rev. B* **2003**, 68, 195116.

von-Neumann-type single-orbital entropy

$$s(1)_i = - \sum_{\alpha=1}^4 \omega_{\alpha,i} \ln \omega_{\alpha,i} \quad (75)$$

($\omega_{\alpha,i}$ is an eigenvalue of the RDM of spatial orbital i — states defined on all other orbitals of the CAS have been traced out)

Entanglement Measures for Embedded Subsystems

- Measure for the entanglement of orbital i **and** orbital j with the environment:

von-Neumann-type two-orbital entropy

$$s(2)_{ij} = - \sum_{\alpha=1}^{16} \omega_{\alpha,ij} \ln \omega_{\alpha,ij} \quad (76)$$

($\omega_{\alpha,ij}$ is an eigenvalue of the RDM of two spatial orbitals i and j — states defined on all other orbitals of the CAS have been traced out)

Entanglement Measures for Embedded Subsystems

- $s(2)_{ij}$ contains also the 'on-site' entropies for the two orbitals
- ⇒ Subtract these contributions to obtain the 'inter-orbital entropy':

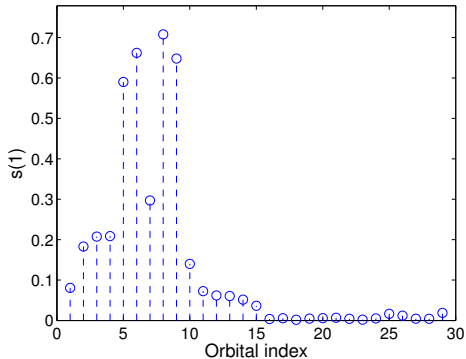
J. Rissler, R.M. Noack, S.R. White, *Chem. Phys.* **2006**, 323, 519.

Mutual information

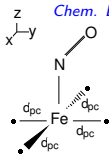
$$I_{ij} \propto s(2)_{ij} - s(1)_i - s(1)_j \quad (77)$$

- Successfully applied to optimize orbital ordering and to enhance DMRG convergence by Ö. Legeza

Entanglement and Orbitals — Single Orbital Entropy



K. Boguslawski, P. Tecmer, Ö. Legeza, M. Reiher, *J. Phys.*

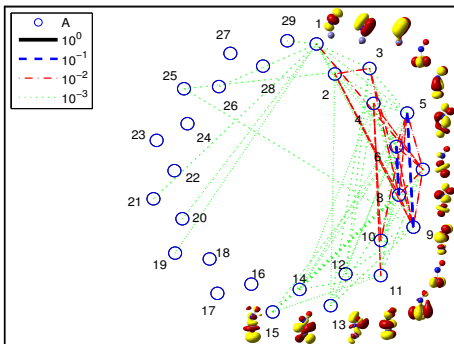


Chem. Lett. **2012**, 3, 3129.

- 4 point charges in xy -plane at $d_{pc} = 1.133 \text{ \AA}$
- Natural orbital basis: CAS(11,14)SCF/cc-pVTZ
- DMRG(13,29) with DBSS ($m_{\min} = 128$, $m_{\max} = 1024$)

- Three groups of orbitals
 - \Rightarrow large single orbital entropy
 - \Rightarrow medium single orbital entropy
 - \Rightarrow (very) small single orbital entropy
- Configurations with occupied orbitals belonging to the third block have small C_I coefficients
 - \Rightarrow Important for dynamic correlation

Entanglement and Orbitals — Mutual Information



- Three groups of orbitals
 \Rightarrow **high entanglement**
 \Rightarrow **medium entanglement**
 \Rightarrow **weak entanglement**
- Strong entanglement for pairs:

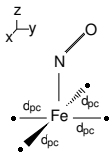
$$(d, \pi^*) \Longleftrightarrow (d, \pi^*)^*$$

$$\pi \Longleftrightarrow \pi^*$$

$$\sigma_{\text{Metal}} \Longleftrightarrow \sigma_{\text{Ligand}}$$

K. Boguslawski, P. Tecmer, Ö. Legeza, M. Reiher, *J. Phys.*

Chem. Lett. **2012**, 3, 3129.



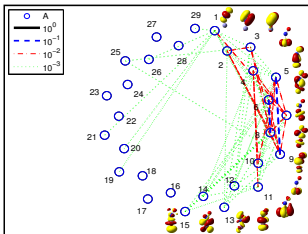
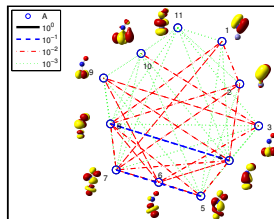
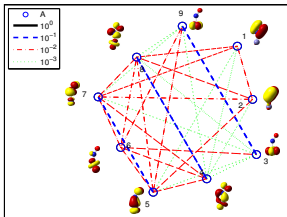
- 4 point charges in xy -plane at $d_{\text{pc}} = 1.133 \text{ \AA}$
- Natural orbital basis: CAS(11,14)SCF/cc-pVTZ
- DMRG(13,29) with DBSS ($m_{\text{min}} = 128$, $m_{\text{max}} = 1024$)

\Rightarrow Important for **static** and **nondynamic** correlation (\Longleftrightarrow chemical intuition of constructing a CAS)

Artifacts of Small Active Space Calculations

Comparison of DMRG(11,9)[220] and DMRG(11,11)[790] to

DMRG(13,29)[128,1024,10⁻⁵] for [Fe(NO)]²⁺



- I_{ij} (and $s(1)_i$) overestimated for small active spaces

⇒ Entanglement of orbitals too large

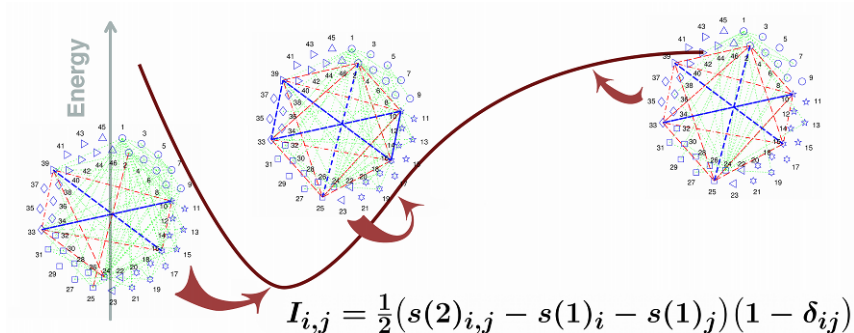
⇒ Missing dynamic correlation is captured in an artificial way

Entanglement and Correlation Effects in Chemical Bonding

- Mutual information I_{ij} and single orbital entropy $s(1)_i$ can serve as **measures of correlation effects**:
 - Dynamic correlation: large number of configurations with small (absolute) weights
⇒ can be captured by including orbitals with small $s(1)_i$ and I_{ij}
 - Static correlation: emerges from nearly degenerate orbitals
⇒ can be captured by including orbitals with large $s(1)_i$ and I_{ij}
- ⇒ **Gradual transition between both correlation effects** is encoded in medium-valued I_{ij} and $s(1)_i$
- ⇒ A **balanced active space can be defined** by entanglement measures to uncover (the most important) static and dynamic correlation

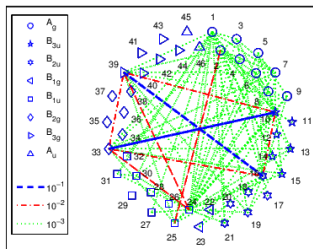
K. Boguslawski, P. Tecmer, Ö. Legeza, M. Reiher, *J. Phys. Chem. Lett.* **2012**, 3, 3129.

Entanglement Measures can Monitor Bond Breaking/Formation Processes: Dinitrogen

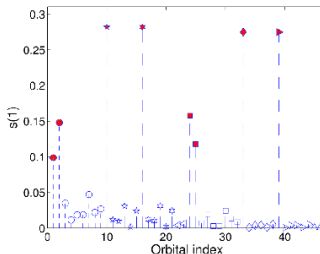


K. Boguslawski, P. Tecmer, G. Barcza, O. Legeza, M. Reiher, *J. Chem. Theory Comput.* **9** 2013 2959–2973 [arxiv: 1303.7207]

Bond Breaking in Dinitrogen at 1.12 Ångström

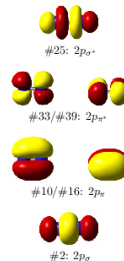


Mutual information



Single orbital entropy

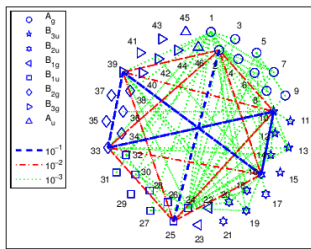
(a) $d_{\text{NN}} = 1.12 \text{ \AA}$



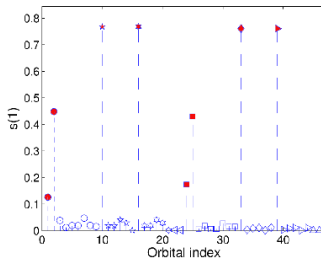
Part of entanglement is already encoded in molecular orbitals changing with the structure !

Atomic-like non-orthogonal basis fcts. exhibit large entanglement measures among each other.

Bond Breaking in Dinitrogen at 1.69 Ångström

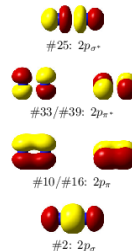


Mutual information



Single orbital entropy

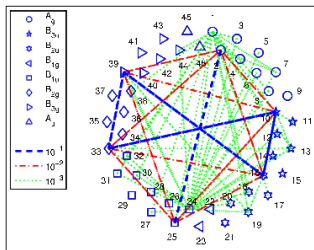
$$(b) d_{\text{NN}} = 1.69 \text{ \AA}$$



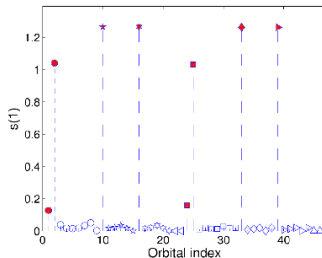
Part of entanglement is already encoded in molecular orbitals changing with the structure !

Atomic-like non-orthogonal basis fcts. exhibit large entanglement measures among each other.

Bond Breaking in Dinitrogen at 2.22 Ångström

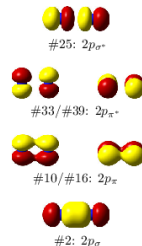


Mutual information



Single orbital entropy

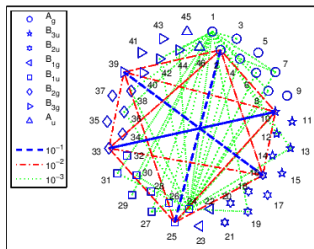
$$(d) d_{\text{NN}} = 2.22 \text{ \AA}$$



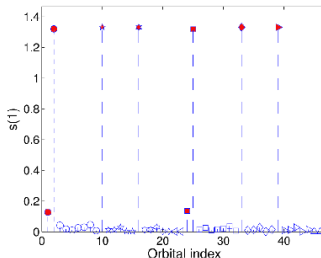
Part of entanglement is already encoded in molecular orbitals changing with the structure !

Atomic-like non-orthogonal basis fcts. exhibit large entanglement measures among each other.

Bond Breaking in Dinitrogen at 3.18 Ångström

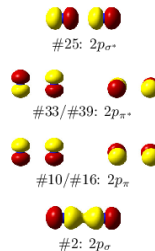


Mutual information



Single orbital entropy

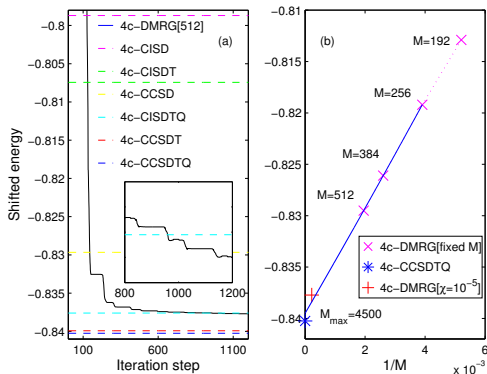
$$(f) d_{\text{NN}} = 3.175 \text{ \AA}$$



Part of entanglement is already encoded in molecular orbitals changing with the structure !

Atomic-like non-orthogonal basis fcts. exhibit large entanglement measures among each other.

'Fully-Relativistic' Four-Component DMRG: TIH



| method | r_e Å | ω_e $\frac{1}{cm}$ | $\omega_e x_e$ $\frac{1}{cm}$ |
|-------------------------|------------|------------------------------|----------------------------------|
| 4c-DMRG(14,94)[512] | 1.873 | 1411 | 26.64 |
| 4c-CISD(14,94) | 1.856 | 1462 | 23.11 |
| 4c-CISDTQ(14,94) | 1.871 | 1405 | 20.11 |
| 4c-MP2(14,94) | 1.828 | 1546 | 47.27 |
| 4c-CCSD(14,94) | 1.871 | 1405 | 19.36 |
| 4c-CCSD(T)(14,94) | 1.873 | 1400 | 23.52 |
| 4c-CCSDT(14,94) | 1.873 | 1398 | 22.28 |
| 4c-CCSDT(Q)(14,94) | 1.873 | 1397 | 21.01 |
| 4c-CCSDTQ(14,94) | 1.873 | 1397 | 22.24 |
| CCSD(T) ^a | 1.876 | 1385 | n/a |
| CCSD(T) ^b | 1.877 | 1376 | n/a |
| MRD-CI ^c | 1.870 | 1420 | n/a |
| SO-MCQDPT ^d | 1.876 | 1391 | 29.42 |
| experiment ^e | 1.872 | 1390.7 | 22.7 |

^a 4c-DC CCSD(T) [14 electrons], Visscher et al. 2001.

^b 4c-DC-Gaunt CCSD(T) [36 electrons], Visscher et al. 2001.

^c GRECP spin-orbit MRD-CI, Titov et al. 2000.

^d model-core potential spin-orbit MCQDPT, Zeng et al. 2010.

S. Knecht, Ö. Legeza, M. Reiher, *J. Chem. Phys.* **140** (2014) 041101

Recent Developments in QC-MAQUIS 1: DFT-embedding for MPO-DMRG

DMRG embedded into a quantum environment

Energy decomposition into system and (spectator) environment

$$E_{\text{tot}} = E_{\text{act}}^{\text{DMRG}} + E_{\text{env}}^{\text{KS-DFT}} + E_{\text{int}}^{\text{OF-DFT}}$$

with

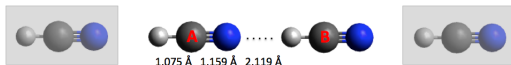
$$E_{\text{act}}^{\text{DMRG}} = \langle \Psi^{\text{act}} | \hat{H}_{\text{act}} | \Psi^{\text{act}} \rangle$$

and

$$E_{\text{int}}^{\text{OF-DFT}}[\rho_{\text{act}}, \rho_{\text{env}}] = T_{\text{s}}^{\text{nad}}[\rho_{\text{act}}, \rho_{\text{env}}] + \\ E_{\text{xc}}^{\text{nad}}[\rho_{\text{act}}, \rho_{\text{env}}] + E_{\text{elstat}}^{\text{int}}[\rho_{\text{act}}, \rho_{\text{env}}]$$

T. Dresselhaus, J. Neugebauer, S. Knecht, S. Keller, Y. Ma, M. Reiher, *J. Chem. Phys.* **142** 2015 044111

DMRG embedding: Dipole moment of a HCN chain



Dipole moment μ in Debye per HCN molecule.

| Method | Active fragment(s) | Env. | μ (per HCN) |
|-----------------------|--------------------|------|--------------------|
| <i>monomer</i> | | | |
| DMRG(10,9)[4096]-SCF | A | — | 3.09 |
| DFT | A | — | 2.96 |
| DMRG(10,9)[4096]-SCF | A | DFT | 3.54 |
| DFT | A | DFT | 3.42 |
| DMRG(10,9)[4096]-SCF | B | DFT | 3.43 |
| DFT | B | DFT | 3.32 |
| <i>dimer</i> | | | |
| DMRG(20,18)[4096]-SCF | A+B | — | 3.44 |
| DMRG(20,18)[4096]-SCF | A+B | DFT | 3.91 |
| DFT | A+B | DFT | 3.93 |
| <i>tetramer</i> | | | |
| DMRG(40,36)[2048]-SCF | all | — | 3.81 |

T. Dresselhaus, J. Neugebauer, S. Knecht, S. Keller, Y. Ma, M. Reiher,
J. Chem. Phys. 142 2015 044111 (Erratum: *ibid.* 189901)

Recent Developments in QC-MAQUIS 2: Dynamic Correlation through DFT

Dynamic correlation through short-range DFT

Decomposition into active and inactive system

$$E_{\text{CAS-Cl}} = E_{\text{I}} + E_{\text{A}}$$

where

$$E_{\text{I}} = \frac{1}{2} \sum_{ij} (h_{ij} + f_{ij}^{\text{I}}) D_{ij}^{\text{I}} + V_{\text{nn}} = \sum_i (h_{ii} + f_{ii}^{\text{I}}) + V_{\text{nn}}$$

$$E_{\text{A}} = \sum_{uv} f_{uv}^{\text{I}} D_{uv}^{\text{A}} + \frac{1}{2} \sum_{uvxy} g_{uvxy} P_{uvxy}^{\text{A}}$$

with

$$f_{pq}^{\text{I}} = h_{pq} + \sum_k (2g_{pqkk} - g_{pkqk})$$

and

$$g_{pqrs} = \langle \phi_p(\mathbf{r}_1) \phi_r(\mathbf{r}_2) | \hat{g}(1, 2) | \phi_q(\mathbf{r}_1) \phi_s(\mathbf{r}_2) \rangle$$

Dynamic correlation through short-range DFT

Introduce the range separation into the electron–electron interaction

$$\hat{g}(1, 2) = \hat{g}^{\mu,lr}(1, 2) + \hat{g}^{\mu,sr}(1, 2)$$

with

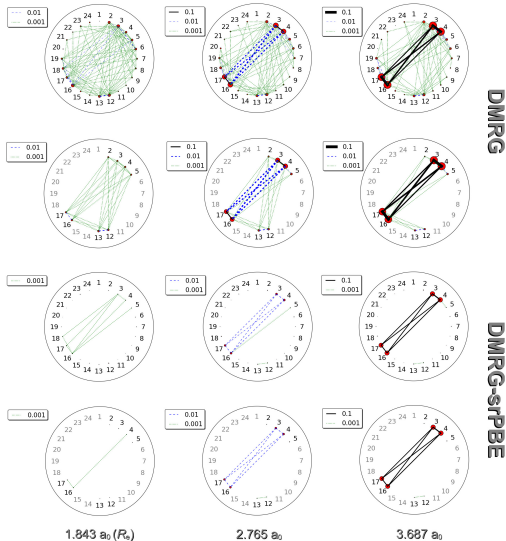
$$\hat{g}^{\mu,lr}(1, 2) = \frac{\text{erf}(\mu|\mathbf{r}_1 - \mathbf{r}_2|)}{|\mathbf{r}_1 - \mathbf{r}_2|}$$

$$\hat{g}^{\mu,sr}(1, 2) = \frac{1 - \text{erf}(\mu|\mathbf{r}_1 - \mathbf{r}_2|)}{|\mathbf{r}_1 - \mathbf{r}_2|}$$

Then, the energy can be set up as

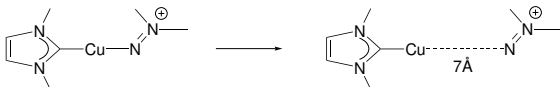
$$E_{\text{CAS-Cl}}^{\text{srDFT}} = E_{\text{I}}^{\text{lr}} + E_{\text{A}}^{\text{lr}} + E_{\text{H}}^{\text{sr}}[\rho] + E_{\text{xc}}^{\text{sr}}[\rho]$$

Regularizing effect of srDFT on small CAS: Water



E. D. Hedegård, S. Knecht, J. S. Kielberg, H. J. A. Jensen, and M. Reiher, *J. Chem. Phys.* 142 2015 224108

DMRG–srDFT for the WCCR10 test set



Calculated dissociation energies in kJ/mol

| Method | D_e (kJ/mol) | D_0 (kJ/mol) |
|---|----------------|----------------|
| DMRG[2000](30,22) | 173.5 | 165.1 |
| DMRG[2000](20,18) | 169.9 | 161.5 |
| DMRG[2000](10,10) | 132.8 | 124.3 |
| DMRG[2000](30,22)-srPBE | 225.1 | 216.6 |
| DMRG[2000](20,18)-srPBE | 227.9 | 219.4 |
| DMRG[2000](10,10)-srPBE | 216.5 | 208.0 |
| PBE | 240.2 | 231.8 |
| PBE (full complex/def2-TZVP) | 257.5 | 249.0 |
| PBE (full complex/def2-QZVPP from WCCR10) | 247.5 | 239.0 |
| Exp. (from WCCR10) | 226.7 | 218.2 |

E. D. Hedegård, S. Knecht, J. S. Kielberg, H. J. A. Jensen, and M. Reiher, *J. Chem. Phys.* **142** 2015 224108;
WCCR10: T. Weymuth, E. P. A. Couzijn, P. Chen, M. Reiher, *J. Chem. Theory Comput.* **10** 2014 3092